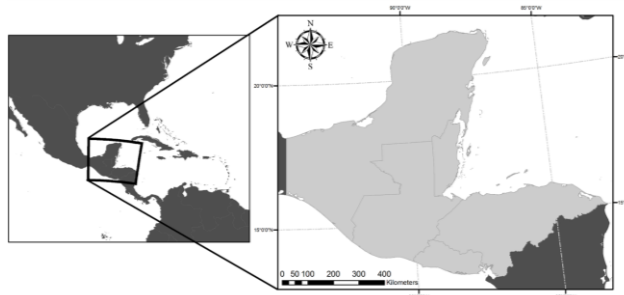


Amanda Weigel\* and Dr. Robert Griffin  
University of Alabama in Huntsville, Huntsville, Alabama

### 1. INTRODUCTION

The Yucatán region spans across portions of Mexico, Guatemala, Honduras, El Salvador, and Belize (Figure 1). Historically, this region has proven to have an active tropical climatology as it has been hit by numerous large scale, high magnitude hurricanes. Paleo-climatological evidence has dated hurricane activity back 5,000 years through sediment core sampling taken from low energy water bodies along coastal Belize (McCloskey and Keller, 2008). Recently, this region has been affected by high magnitude storms including Hurricane Mitch, Keith, Dean, and Andrew, which caused recording breaking flooding, billions of dollars in damages, and over 10,000 fatalities (IFRC, 2000; NOAA, 2009). Tropical activity in the past century has demonstrated this area to be extremely susceptible to hurricanes.

Because the Yucatán regions spans across portions of five countries with varying economic statuses and political policies, it is difficult to assess the risk of hurricane induced hazards throughout this area as detailed historical and predictive atmospheric model data is unavailable. This work presents a methodology for using a Geographic Information System (GIS) to combine various layer components for analysis of susceptibility to hurricane hazards using recorded hurricane information, and land surface characteristics.



**Figure 1: Study area map depicting the Yucatán Region**

---

*Corresponding author address:* Amanda Weigel,  
Univ. of Alabama in Huntsville, Dept. of Atmospheric  
Science, Huntsville, AL; 35805 e-mail:  
amweigel@nssc.uah.edu

### 1.1 HURRICANE HAZARDS

Hurricane hazards selected for this analysis include the common hurricane hazards: high winds, storm surge flooding, and non-storm surge flooding (NOAA, 1999). Additionally, rainfall triggered landslides were selected as the fourth hazard since portions of the study area are prone to landslides as numerous related damages and deaths have been reported from past hurricanes.

### 2. DATA AND PRE-PROCESSING

Data sets selected for this analysis were determined based on a balance between their geographic coverage, spatial resolution, data size, and processing time. Table 1 outlines all datasets and their associated spatial resolution, temporal, and geographic coverage.

The Global Administrative Areas (GADM) dataset provides fine resolution global country boundaries. For this analysis GADM was selected to derive the extent of the study area because it provided the finest resolution data of global coastlines.

Hurricane track data was acquired from the National Oceanic and Atmospheric Administration (NOAA) National Climatic Data Center. The International Best Track Archive for Climate stewardship (IBTrACS) hurricane tracks were selected for this analysis due to its availability in a variety of GIS compatible formats, its endorsement by the World Meteorological Organization Tropical Cyclone Programme, and its detailed data on an array of hurricane parameters for storms dating back to 1851. Storms used for this analysis were condensed to a time period from 1970-2011 since hurricane tracks recorded prior to the 1970s are considered less accurate because weather observation methods, particularly satellites, were not available to provide a real time method for monitoring storm conditions (Davis, 2011).

Shuttle Radar Topography Mission (SRTM) data was selected as the topographic dataset and acquired from the USGS Earth Explorer data distribution site. SRTM data files were mosaicked together, masked to remove erroneous data ranges, filled to remove sinks, and corrected by removing negative elevation.

Dataset	Spatial Resolution	Temporal Coverage	Geographic Coverage
International Best Track Archive for Climate Stewardships ( <b>IBTrACS</b> ) Hurricane tracks	n/a	1851-2011	Global
Global Administrative Boundaries ( <b>GADM</b> )	n/a	2010	Global
Shuttle Radar Topography Mission ( <b>SRTM</b> ) Digital Elevation Model	90 m	2001	Global
USGS Hydrological data and maps based on Shuttle Elevation Derivatives at multiple Scales ( <b>HydroSHEDS</b> ) River Locations	~500 m	2007	Global (excluding poles)
<b>WorldClim</b> monthly accumulated precipitation	~1 km	1950-Present	Global
Harmonized World Soil Database	~1 km	2012	Global

**Table 1: Data set information**

River network locations were acquired from the USGS Hydrological data and maps based on Shuttle Elevation Derivatives at multiple Scales (HydroSHEDS) data, which provides global hydrographic information derived from SRTM data for regions where it is unavailable. River network shapefiles for Central America were acquired at 15 arc-second resolution and clipped down to the extent of study area.

The Harmonized World Soil Database is a collaboration between ISRIC, the European Soil Bureau Network, and the Institute of Soil Science, Chinese Academy of Sciences to combine and make soil information available globally. Soil type data was acquired for the Yucatán region at 30 arc-second resolution.

Accumulated monthly precipitation data was collected at 30 arc-second resolution from the WorldClim data redistribution site to assess rainfall quantity and distribution. Data was collected for the span of the North Atlantic hurricane season from June 1<sup>st</sup> through November 30<sup>th</sup>.

### 3. METHODOLOGY

Methods used to assess the risk of hurricane induced hazards were adopted from Vahrson (1994) and SERVIR (2012). For each hazard, a set of underlying susceptibility factors were determined based on previous methodologies from literature. Susceptibility factors were then rescaled, and plugged into their associated hazard equation. Table 2 outlines each hazard, the determined susceptibility factors, and the hazard equations.

#### 3.1 HIGH WIND

Maximum winds within a hurricane occur in a region called the radius of maximum wind (RMW) located just outside the eye wall, and varies in distance from the center depending on the strength and diameter of the storm's eye (Bettinger, Merry, and Kepinstall, 2009). On average, the RMW occurs approximately 50 km from the storm's center (NOAA, 1999), where several hurricane radial wind profile studies have modeled hurricane wind speeds peaking near this distance (Wood et al., 2012; Holland, Belanger and Fritz, 2010; Wang and Rosowsky, 2012; Vickery et al. 2009; Taramelli et al. 2013). Hurricane data were reduced to 75 storms passing within 50km of the study area, a distance representative of the generalized location for the RMW.

A model was created using ArcGIS Model Builder to map the temporal radial wind profile of each storm. The hurricane wind profile model iterated through hurricane track and applied the Euclidean Distance tool to map a continuous hurricane extent using a generalized radius of 250km based on previous studies (Wood et al., 2012; Holland, Belanger and Fritz, 2010; Wang and Rosowsky, 2012; Vickery et al. 2009; Taramelli et al. 2013; NOAA, 1991). A spatial resolution of 10km was selected to manage processing time. In order to map the radial wind distribution of each hurricane, a fuzzy membership function was applied to each storm extent dataset using the small function as it provided a line of best fit to hurricane wind profiles. The function was controlled by starting at the center of the storm, setting the peak value at 50km out to represent the RMW, and then setting 250km as the spread to go towards zero, since the hurricane wind

Hazard	Susceptibility Factors	Variable	Scale	Hazard Equation
Wind	Wind Speed	$Sw_v$	0-1	$H_{Wind} = Ave(Sw_v \times Sd \times Sw_d)$
	Distance from Eye	$Sd$	n/a	
	Radial Wind Distribution	$Sw_d$	n/a	
Storm Surge Flooding	Onshore Wind Speed	$Sw_{vo}$	0-1	$H_{Surge} = (Sw_{vo} \times Se_c)$
	Low Lying Coastal Elevations	$Se_c$	1-0	
Non-Storm Surge Flooding	Elevation Above Drainage	$Se_d$	1-0	$H_{Flood} = (Se_d \times Sf \times Sv)$
	Storm Frequency	$Sf$	0-1	
	Storm Velocity	$Sv$	1-0	
Rainfall Triggered Landslides	Soil Type	$Sl$	0-5	$H_{Land} = (Sr \times Sl \times Sh)(Sf_r \times Sv_r)$
	Slope	$Sr$	0-5	
	Soil Humidity	$Sh$	1-5	
	Storm Frequency Rescaled	$Sf_r$	1-5	
	Storm Velocity Rescaled	$Sv_r$	1-0	

**Table 2: Hurricane hazard susceptibility factors and hazard equations**

speed drastically decreases with distance from the eye.

It was necessary to account for the temporal change in wind speed since hurricanes are dynamic systems, changing in strength as they move over different surface conditions. Incremental wind speed measurements were attributed to the radial wind. A 10km fishnet covering the extent of the 50km distance from the coastline was created at a resolution, then snapped to a template raster to insure all pixels align in final processing. A near table was then generated to identify grid cells closest to the segmented portion of each hurricane track measurement. The hurricane track data was then joined to the near table to attribute maximum sustained wind speed values to cells found closest to the track. The near table was again joined to the original 10km fishnet and exported to a new shapefile before being converted to raster format. The resulting raster file covered the extent of the fishnet, containing segmented areas attributed to maximum sustained wind speed values.

Two components were used to assemble the final wind profile: the generated fuzzy membership raster file and the raster conversion of the near table-fishnet join. Raster calculator was used to attribute wind speed values to the fuzzy membership wind speed distribution file by multiplying the two files together. Fuzzy membership values range on a scale from zero to one, with one closer to the storm center at the location of the RMW, and zero at a distance of 250km where the edge of the storm is defined. Raster files representing the temporal change in maximum sustained wind speed were multiplied by the weighted fuzzy membership function wind speeds values. The resulting wind distribution values are distributed so that fuzzy membership

values originally set to one equal the maximum sustained wind speed, and outer values gradually decrease to zero as a function of the small function.

To identify areas most at risk of experiencing high winds, the average wind speed and frequency of hurricane occurrence were assessed. This was done through the use of Cell Statistics to average the wind profiles for all 75 storms to calculate the per pixel average wind speed. From the calculated average, a Wind Speed Impact Factor was created by rescaling average wind speed values from 0-1. Areas closer to one have a higher risk of experiencing high wind speeds from hurricanes.

### 3.2 STORM SURGE FLOODING

To model storm surge, three factors were considered: onshore wind speed, frequency of occurrence, and low lying coastal elevations. Storm surge is highly dependent on the strength of hurricane winds particularly on the right side of the storm where the counter clockwise rotation pushes water towards the coastline yielding higher water depths (Ozcelik, Gorokhovich, and Doocy, 2012). To model onshore wind speed, the Wind Profile Model was adopted to only focus on the right side of the storm. Cell Statistics were then used to derive the per pixel average wind speed, before rescaling values from 0-1.

Low-lying coastal areas were extracted from SRTM data for areas with elevations up to four meters, separated into four raster files with elevation ranges in one meter increments. Darson, Asmath and Jehu (2013), Wang et al. (2011) and Kleinosky, Yarnal and Fisher (2006) used GIS to map storm surge and sea level rise in coastal regions where the study area is either small, or the

extracted inundation levels are limited to a certain inland distance. However, due to a significant portion of the study area extent consisting of low lying inland areas, low-lying coastal elevations needed to be extracted, and were done so using maximum recorded storm surge depths from damage reports (Avila, 2001; NOAA, 2009). Additionally, it was necessary to remove isolated low-lying areas where onshore water would not be able to flow inland due to obstructing terrain. To accomplish this, Feature Selection by Location was used to identify low elevation features within each converted elevation polygon that came in contact with the GADM coastline. Identified areas were merged into a single shapefile consisting of all four coastal inundation levels, and then inversely scaled from 1-0 so that coastal regions were weighted higher than more inland elevations as they are less prone to storm surge flooding.

To identify storm surge risk, scaled elevation ( $Se_c$ ) and wind speed impact factors ( $Sw_{vr}$ ) were multiplied together according to the Surge Hazard equation in Table 2 to locate areas where both high winds and low elevations overlap. Resulting values range from 0-1, with one identifying regions of highest risk, and zero with lowest risk.

### 3.3 NON-STORM SURGE FLOODING

A major hurricane hazard resulting from heavy rainfall rates is flooding. Flood depths depend on the elevation of a given area, its relationship to drainage areas, and the frequency of hurricane occurrence, and its storm velocity.

To identify elevations above drainage areas, a Height Above Nearest Drainage (HAND) Model was applied to SRTM elevation data using methods described by Rennó et al. (2008) and Nobre et al. (2011). Flow direction was obtained from SRTM data using the Flow Direction tool in ArcGIS. To provide a baseline drainage height, river elevations needed to be extracted from the USGS HydroSHEDS stream locations. Stream locations were first converted to a raster dataset using the Polyline to Raster tool, and then used as a mask to extract the elevation value for each pixel of the river locations. The extracted river elevations and flow direction were used to delineate watersheds using the Watershed tool, which identifies cells that flow into separate river drainage locations, outputting watershed values representative the river elevation value of which areas flow into. The watershed values were subtracted from the initial SRTM elevation, outputting a raster file with elevation ranges where drainage locations are set as zero, yielding heights

above drainage. Elevations ranging from 0-5m based on historic non-storm surge related flooding reports were extracted and inversely rescaled from 1-0 so that lower elevations were weighted higher (Beven, 2001; IFRC, 2000; NOAA, 2009).

The velocity a hurricane moves affects the amount of precipitation deposited over a given area. Slower moving hurricanes deposit more precipitation than faster moving storms because more time is allowed to deposit precipitation over an area, resulting in higher rainfall totals. Each hurricane track is formatted as a series of line segments connecting hurricane data collection points are six hour intervals. To calculate each storm's velocity, the distance between collection points was calculated and then divided by the time interval to identify the temporal change in storm velocity in meters per second. The wind hazard model was then adapted to model the extent and change in velocity for each of the 75 storms, assuming the entirety of the hurricane travels at the same rate. Finally, storm velocity model results were averaged using Cell Statistics to assess per 10km pixel, the average storm velocity based on the number of storms experienced by the areas. Values were then scaled inversely from 0-1 so that lower velocities were weighted higher because they are more indicative of flooding.

Storm frequency was calculated by mapping the extent of each storm using a generalized 250km radius, then summed over the study area to calculate the frequency of hurricane occurrence per pixel. Values were then rescaled from 0-1. To identify non-storm surge flooding, an impact factor was created by combining susceptibility factors following the Flood Hazard Equation in Table 2 were  $Se_d$  is elevations above drainage,  $Sf$  is storm frequency, and  $Sv$  is storm velocity.

### 3.4 RAINFALL TRIGGERED LANDSLIDES

This hazard assessment identifies landslides that are triggered by hurricane induced rainfall. High rain fall saturates the soil, reducing the friction which keeps debris stationary on a surface. This analysis adopts methods used by Vahrson (1994) and NASA SERVIR (2012) to identify areas likely to experience hurricane rainfall triggered landslides using six factors: soil type, slope, soil humidity, storm frequency, and storm velocity.

Slope values for the Yucatán region were derived from the SRTM DEM and reclassified from 0-5 using intervals proposed by SERVIR (2012). Areas with steep slopes are more prone to debris flow than areas with shallow slopes, thus higher slopes were classified closer to five.

Soil information from the Harmonized World Soils database contained soil type and characteristic information. Individual soil types were classified on a 1-5 scale ranging from low to very high susceptibility values as defined by Vahrson (1994) and professional knowledge of a consulting soil scientist.

Increases in water raise the failure likelihood of soils by increasing pore pressure (Vahrson, 1994), thus it is necessary identify areas with high soil moisture during the hurricane season where increases in water content make it vulnerable to landslides. Soil humidity was assessed by classifying average monthly precipitation values on a 0-2 scale using indices specified by Vahrson (1994). These soil moisture values were then summed by the index values for each of the five months and divided equally into five index factor classes.

To account for areas that are most commonly hit by hurricanes, storm frequency calculated previously was used, however values were rescaled from 1-5 to match the scales used for the other factors. Areas experiencing the highest frequency of hurricane events were weighted the highest.

Storm velocity is an indicator on the amount of rainfall deposited over an area from a hurricane, so areas experiencing more rainfall are more likely to trigger landslide events. Storm velocity values calculated using the methods described for non-storm surge flooding were rescaled inversely from 5-1 in agreement with the other hazard mapping index values. Storm velocity was inversely scaled so areas that have experienced slower moving storms were weighted higher than areas experience fast moving storms.

To identify areas likely to experience rainfall triggered landslides the landslide hazard equation in Table 2 was adopted to assess hurricane rainfall triggered landslide. The equation originally multiplied the susceptibility factors of lithology ( $S_l$ ), slope ( $S_r$ ), and soil humidity ( $S_h$ ) by seismic triggering factors. Since this analysis examines hurricane rainfall triggers, seismic triggers we substituted for storm frequency ( $S_f$ ) and storm velocity ( $S_v$ ) and multiplied by the other susceptibility factors. The resulting raster file was rescaled from 0-1 to generate a Landslide Impact

Factor where areas closer to one are most likely to experience landslides.

#### **4. RESULTS AND DISCUSSION**

This analysis found the eastern side of the peninsula, primarily coastal Belize and Mexico, at greatest risk of experiencing hurricane hazards. Figures 2-5 display the results of the hurricane hazard analysis. Figure 2 depicts high wind risk highest along coast areas of the Yucatán Peninsula. Similarly, storm surge (Figure 3) and non-storm surge (Figure 4) flooding are also highest along these coastal areas, particularly where there is low lying elevation.

Figure 5 depicts landslide risk to be highest in the southeastern portion of the study area. Unlike the previous three hazards, landslide risk is higher in the southeast due to increased terrain variability, and slower storm motion resulting from its greater land area.

#### **5. CONCLUSIONS**

This work succeeded in mapping hurricane hazards, obtaining results indicative of those expected from previous hurricane damage reports. Novel methodologies developed from this analysis can be adapted for further risk assessment on hurricane prone areas that lack predictive model data for a detailed analysis. The developed methods may also be applied to enhance current hazard mapping techniques in areas that have more data available. Future work in this area involves validating methodologies by geographically comparing data on past hazard events to calculated risk.

#### **6. ACKNOWLEDGEMENTS**

I would like to thank Dr. Nicholas Dunning from the University of Cincinnati for his expertise in classifying soil types. To Mr. Eric Anderson from NASA SERVIR for his help developing hazard mapping methodologies. And finally, to the University of Alabama in Huntsville Earth System Science Center and Department of Atmospheric Science for providing the necessary computing power, software, and facilities that made this research possible.

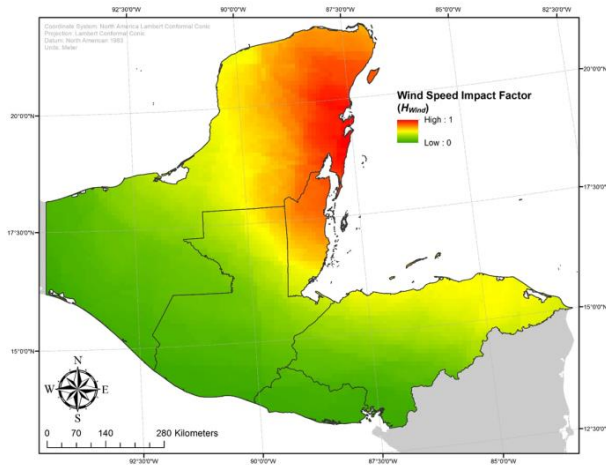


**Figure 2: Wind Speed Impact Factor**

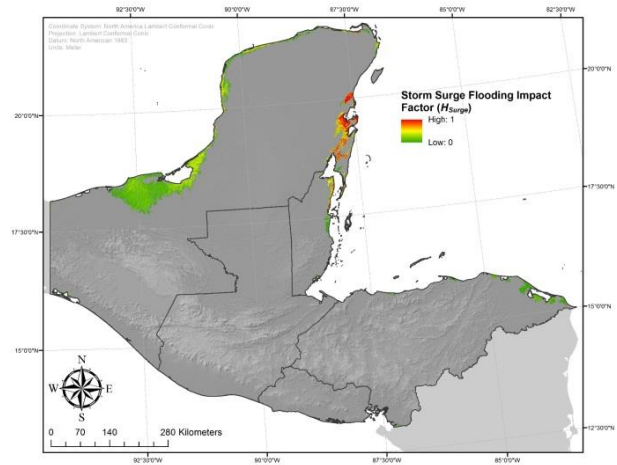


**Figure 3: Storm Surge Flooding Impact Factor**

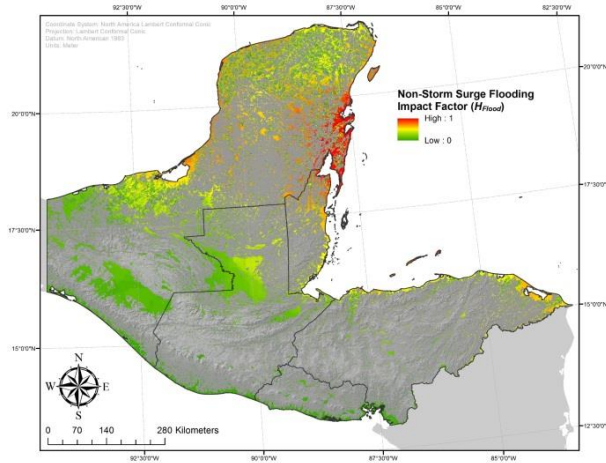


**Figure 4: Non-Storm Surge Flooding Impact Factor**

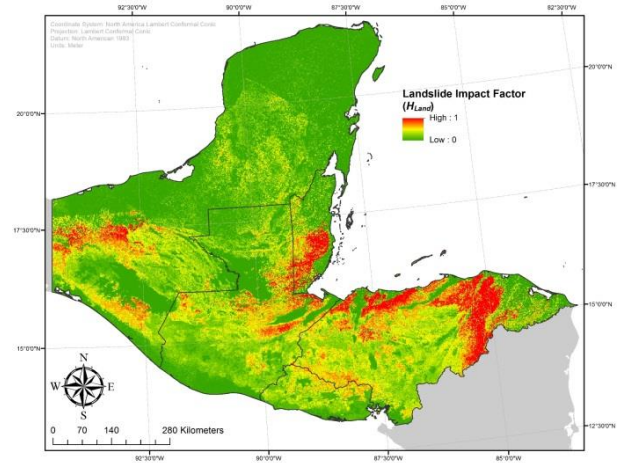


**Figure 5: Landslide Impact Factor**

## 7. REFERENCES

- Avila, Lixion, A., 2001: Tropical Cyclone Report Hurricane Iris 4-9 October 2001, National Hurricane Center. Retrieved [http://www.nhc.noaa.gov/data/tcr/AL112001\\_Iris.pdf](http://www.nhc.noaa.gov/data/tcr/AL112001_Iris.pdf)
- Bettinger, P., Merry, K., & Hepinstall, J., 2009: Average tropical cyclone intensity along the Georgia, Alabama, Mississippi, and north Florida coasts. *southeastern geographer*, 49(1), 50-66.
- Beven, Jack, 2001: Tropical Cyclone Report Hurricane Keith 28 September – 6 October 2000. National Hurricane Center. Retrieved [http://www.nhc.noaa.gov/data/tcr/AL152000\\_Keith.pdf](http://www.nhc.noaa.gov/data/tcr/AL152000_Keith.pdf)
- Boose, E. R., Foster, D. R., Plotkin, A. B., & Hall, B., 2003: Geographical and historical variation in hurricanes across the Yucatan Peninsula. *The lowland Maya area*. Haworth. New York, NY, EEUU, 495-516.
- Darsan, J., Asmath, H., & Jehu, A., 2013: Flood-risk mapping for storm surge and tsunami at Cocos Bay (Manzanilla), Trinidad. *Journal of Coastal Conservation*, 17(3), 679-689.
- Holland, G. J., Belanger, J. I., & Fritz, A., 2010: A Revised Model for Radial Profiles of Hurricane Winds. *Monthly Weather Review*, 138(12).
- IFRS, 2000: Belize: Hurricane Keith. Emergency Appeal. Retrieved <http://www.ifrc.org/docs/appeals/00/2900r.pdf>
- Kleinosky, L. R., Yarnal, B., & Fisher, A., 2007: Vulnerability of Hampton Roads, Virginia to



- storm-surge flooding and sea-level rise. *Natural Hazards*, 40(1), 43-70.
- Davis, G., 2011: History of the NOAA Satellite Program. NOAA Satellite and Information Service
- NOAA, 1999: Hurricane Basics (1999). Accessed May 2014 From <http://www.disastersrus.org/MyDisasters/NOAA/hurricanebook.pdf>
- NOAA, 2009: Mitch: The Deadliest Atlantic Hurricane Since 1780. Climate Monitoring, NCDC, NOAA. Retrieved from <https://www.ncdc.noaa.gov/oa/reports/mitch/mitch.html>
- Nobre, A. D., Cuartas, L. A., Hodnett, M., Rennó, C. D., Rodrigues, G., Silveira, A., ... & Saleska, S., 2011: Height above the nearest drainage—a hydrologically relevant new terrain model. *Journal of Hydrology*, 404(1), 13-29.
- Ozcelik, C., Gorokhovich, Y., & Doocy, S., 2012: Storm surge modelling with geographic information systems: estimating areas and population affected by cyclone Nargis. *International Journal of Climatology*, 32(1), 95-107.
- Puotinen, M. L., 2007: Modelling the risk of cyclone wave damage to coral reefs using GIS: a case study of the Great Barrier Reef, 1969–2003. *International Journal of Geographical Information Science*, 21(1), 97-120.
- Rennó, C. D., Nobre, A. D., Cuartas, L. A., Soares, J. V., Hodnett, M. G., Tomasella, J., & Waterloo, M. J., 2008: HAND, a new terrain descriptor using SRTM-DEM: Mapping terra-firme rainforest environments in Amazonia. *Remote Sensing of Environment*, 112(9), 3469-3481.
- SERVIR, 2012: Dynamic Landslide Hazard Mapping in Nicaragua. *National Pilot Application Report Nicaragua, NASA*
- Subramanian, C., Pinelli, J. P., Kostanic, I., & Lapilli, G., 2012: Analysis and Characterization of Hurricane Winds. *Journal of Engineering Mechanics*, 139(3), 325-338.
- Taramelli, A., Meelli, L., Pasqui, M., & Sorichetta, A., 2010: Modelling risk hurricane elements in potentially affected areas by a GIS system. *Geomatics, Natural Hazards and Risk*, 1(4), 349-373.
- Vahrson, W. G., 1994: Macrozonation methodology for landslide hazard determination. *Bulletin-Association of Engineering Geologists*, 49.
- Vickery, P. J., Masters, F. J., Powell, M. D., & Wadhera, D., 2009: Hurricane hazard modeling: The past, present, and future. *Journal of Wind Engineering and Industrial Aerodynamics*, 97(7), 392-405.
- Wang, Y., Li, Z., Tang, Z., & Zeng, G., 2011: A GIS-based spatial multi-criteria approach for flood risk assessment in the Dongting Lake Region, Hunan, Central China. *Water resources management*, 25(13), 3465-3484.
- Wang, Y., & Rosowsky, D. V., 2012: Joint distribution model for prediction of hurricane wind speed and size. *Structural Safety*, 35, 40-51.
- Wood, V. T., White, L. W., Willoughby, H. E., & Jorgensen, D. P., 2013: A New Parametric Tropical Cyclone Tangential Wind Profile Model. *Monthly Weather Review*, 141(6).